Vibrational dynamics of excited electronic states of molecular iodine

A. Scaria, V. Namboodiri, J. Konradi, and A. Materny[a)]
School of Engineering and Science, Jacobs University Bremen, Campus Ring 1, D-28759 Bremen, Germany

(Received 23 May 2007; accepted 5 September 2007; published online 9 October 2007)

Femtosecond degenerate four-wave-mixing spectroscopy following an initial pump laser pulse was used to observe the wave packet dynamics in excited electronic states of gas phase iodine. The focus of the investigation was on the ion pair states belonging to the first tier dissociating into the two ions $I^-(^1S)+I^+(^3P_2)$. By a proper choice of the wavelengths of the initial pump and degenerate four-wave-mixing pulses, we were able to observe the vibrational dynamics of the $B\ ^3\Pi_u^+$ state of molecular iodine as well as the ion pair states accessible from there by a one-photon transition. The method proves to be a valuable tool for exploring higher lying states that cannot be directly accessed from the ground state due to selection rule exclusion or unfavorable Franck-Condon overlap.
 [DOI: 10.1063/1.2790438]

I. INTRODUCTION

Iodine has a number of ion pair states, from where dissociation results in iodine ions not atoms. The first group consists of six ion pair states [$D'(2_g)$, $\beta(1_g)$, $D(0_u^+)$, $E(0_g^+)$, $\gamma(1_u)$, and $\delta(2_u)$], all dissociating into the ions $I^-(^1S)+I^+(^3P_2)$. These closely lying states are around 40 000 cm^{-1} above the ground state and not all of them are easily accessible. The spectroscopic constants and equilibrium internuclear distances of the ion pair states in each tier are similar. Even though extensive work has been done to characterize the ion pair states in the frequency domain, time-resolved investigations are few and far between. Most of the investigations in the time domain were centered around the characterization of the ground state and the readily accessible B state.[1–6] Femtosecond pump-probe spectroscopy based on fluorescence detection was used by Bowman and co-workers to observe the vibrational dynamics of the B state of iodine.[1,2] Schmitt *et al.*[3,4] used femtosecond four-wave-mixing spectroscopy, where three laser pulses interact with the molecular system to produce a nonlinear signal. They studied the vibrational wave packets in the ground as well as excited B states of molecular iodine. By varying the time delay of one of the incident pulses, while keeping the other two pulses fixed, they showed that vibrational dynamics can be observed for both the ground X and excited B states. By introducing two variable time delays, one between the pump and the Stokes pulse and the other between the Stokes pulse and the probe pulse in a coherent anti-Stokes Raman scattering scheme, Knopp *et al.*[5] were able to access higher lying ground vibrational states of molecular iodine. Siebert *et al.*[6] demonstrated that by choosing different polarizations for the three independent laser pulses in the four-wave scheme, a selectivity with respect to the rotational and vibrational dynamics could be achieved for iodine.

The first of the studies investigating femtosecond dynamics of ion pair states was performed by Bowman *et al.*[7] By using multiphoton excitation and depletion techniques they were able to observe contributions from the bound $B\ ^3\Pi_u^+$ and $D(0_u^+)$ states and also from the repulsive $0_g^+(^1\Sigma)$ state of I_2. Farmanara *et al.*[8] used femtosecond pump-probe spectroscopy in the vacuum ultraviolet to excite and observe vibrational wave packets in higher lying ion pair states of iodine. In the aforementioned studies, however, only states of odd symmetry (ungerade) were accessed from the ground state.

Our interest here is to monitor states of even (gerade) symmetry. Excited electronic states of iodine having an even parity cannot be accessed by a single photon transition from the ground state since the ground state ($X\ ^1\Sigma_g^+$) itself has an even parity. To overcome the above problem, we used a combination of an initial pump laser pulse and a time-resolved degenerate four-wave-mixing (DFWM) technique for getting information on the higher lying excited states that are partially not accessible from the ground state due to symmetry reasons. In this scheme, the initial femtosecond pump pulse is used to initiate the dynamics by taking the molecule into an excited state (here, the B state). This excited state possesses odd symmetry, and hence higher lying states of even symmetry could now be probed by using three FWM beams. Motzkus *et al.* replaced the probe in pump-probe spectroscopy by a DFWM process without internal temporal resolution and applied this technique to unimolecular and bimolecular systems in gas phase.[9] They demonstrated the method's advantages in high sensitivity and background-free detection particularly suitable for states that do not allow for fluorescence detection. Here, we would like to combine the advantages offered by the DFWM technique along with the additional benefits of using an initial pump to explore the dynamics of the B state and the ion pair states of even symmetry. In the next section, we will describe briefly the experimental setup used for pump-DFWM spectroscopy.

II. EXPERIMENTAL

The experimental setup used to realize the pump-DFWM scheme was as follows. Femtosecond pulses at a repetition rate of 1 kHz with a center wavelength of around 775 nm

a)Electronic mail: a.materny@jacobs-university.de

were produced by a commercial femtosecond laser system [Clark-MXR Inc., chirped pulse amplifier (CPA)-2010]. The pulses have an average energy of 1 mJ/pulse. The output of the CPA was equally split and was used to pump two optical parametric amplifiers (OPAs) (TOPAS, Light Conversion). The output of one of the OPAs served as the initial pump pulse (IP). The output of the other OPA was split into three equal parts, which formed the three FWM beams. For the experiments, the wavelength of IP was chosen to be 600 nm which is in resonance with the ground state ($X\ ^1\Sigma_g^+$) to B state transition. The wavelength of the FWM excitation was varied between 370 and 410 nm. This is in resonance with the transition from the B state to the lowest group of ion pair states.

The FWM process requires a spatial and, for the start of the experiment, also a temporal overlap of the beams in the sample. The pulses were delayed during the course of the experiment, with respect to each other using computer controlled linear translation stages in Michelson interferometer arrangements. For all the experiments described in the following, two of the pulses of the DFWM process were kept temporally overlapped. For the DFWM we have used the three dimensional forward geometry (folded BoxCARS),[10] which fulfills the phase matching condition and spatially separates the signal enabling a background-free detection. In this geometry, the three beams will pass through the three corners of the front side of a box. After interaction with the sample, the signal emerges out from the fourth corner of the opposite box side. The IP is made to pass through the center of these box sides.

The four beams were focused into the cuvette containing iodine using a lens with focal length of 200 mm. The cuvette was heated to approximately 60 °C to slightly increase the vapor pressure of the sample for a better signal. The spatially separated DFWM signal was filtered by a pinhole. The signal is then collimated using another lens of the same focal length and is finally directed into a single monochromator, and after dispersion is detected using a charge-coupled device camera. Since the signal is of the same wavelength as the incoming FWM beams, extreme care was taken to minimize background due to scattering from the walls of the cuvette. In the following, the results obtained from the experiments will be presented and the advantages of the technique in obtaining molecular information will be discussed.

III. RESULTS AND DISCUSSION

The aim of the present work was to explore the ion pair states in I_2 using femtosecond time-resolved spectroscopy. Pump-DFWM is an ideal technique for this purpose since it gives a background-free signal. The experimental methodology employed to observe the wave packet motion in the ion pair states of molecular iodine is illustrated in Fig. 1. Here, the excited electronic B state serves as an intermediate state for the FWM process. An initial pump pulse in the visible populates the B state. The spectral bandwidth of the femtosecond laser pulses used here exceeds the energy spacing of the vibrational states accessed. Therefore, depending on the wavelength, a wave packet is created in the B state by coherent excitation of vibrational states. The wave packet evolves in time and is interrogated by DFWM in resonance with the B state to ion pair state transition. In this way, the ion pair states of even symmetry are accessed. Now, by introducing an internal temporal delay within the DFWM process, vibrational dynamics of the B state and ion pair state can be monitored. In the following, we show that by using different time orderings in the pump-DFWM process, dynamics in different potential energy surfaces (PESs) can be accessed.

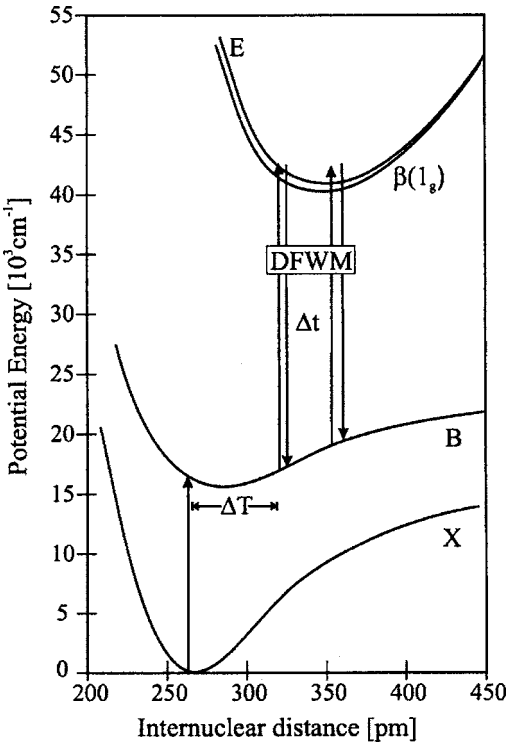

FIG. 1. Potential energy curves of molecular iodine relevant for the present study. Following the selection rules, the states $\beta(1_g)$ and $E(0_g^+)$ are accessible from the excited B state.

In the frequency domain, the ion pair states of iodine have been investigated in great detail.[11–14] With the wavelengths used in our experiments ion pair states belonging to the first tier are accessed. The potential energy curves of these states are similar and the vibrational frequencies are around 100 cm^{-1}. Table I highlights the molecular constants of the B state and the ion pair states of the lowest group correlating with the ions $I^-(^1S)+I^+(^3P_2)$. Not all of these ion pair states are involved due to selection rules. Only the levels

TABLE I. Molecular constants for the excited iodine B state and the ion pair states belonging to the first tier.

State	T_e (cm^{-1})	ω_e (cm^{-1})
$B\ ^3\Pi_0 u^+$	15 641	127
$D'(2_g)$	40 388	104
$\beta(1_g)$	40 821	105
$D(0_u^+)$	41 028	95
$E(0_g^+)$	41 411	101
$\gamma(1_u)$	41 612	95
$\delta(2_u)$	41 789	100

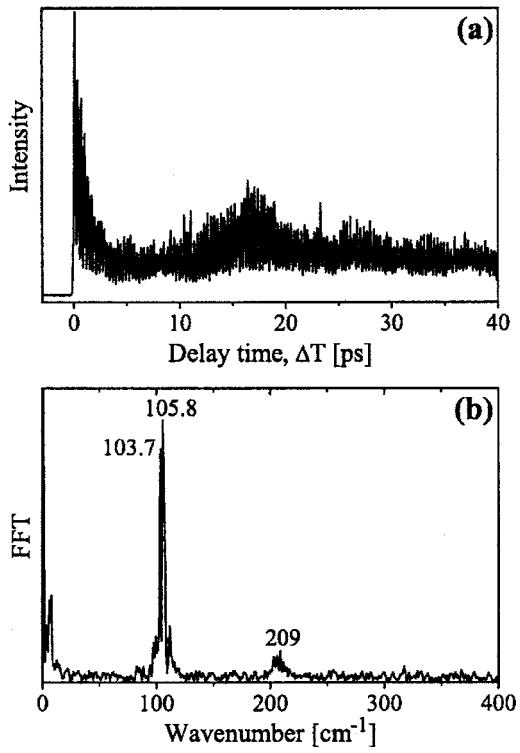

FIG. 2. Panel (a) shows the DFWM signal recorded as a function of the delay time ΔT between the initial pump and the three time-coincident FWM beams. Transients show oscillations with a period of 318 fs. Panel (b) depicts the FFT spectrum of the transient in (a). It shows a peak at approximately 105 cm^{-1}, which corresponds to the vibrational energy spacing of the B state of molecular iodine accessed by the 600 nm laser.

$\beta(1_g)$ and $E(0_g^+)$ are relevant for the present study. The $\beta(1g)$ and $E(0_g^+)$ states have been explored in the earlier experiments performed in the frequency domain by King *et al.*[11] by two photon sequential absorption spectroscopy and also by optical-optical double resonance experiments done by Perrot *et al.*[12]

Here, we present two different kinds of experiments to distinguish the dynamics of the B state and the ion pair states. The first of these experiments is performed to reveal the wave packet dynamics of the B state exclusively. For this, all the DFWM beams are made to arrive simultaneously and the IP is varied relative to the DFWM beams. This is identical to a pump-probe experiment with the probe replaced by a DFWM process. Panel (a) of Fig. 2 shows the transients recorded as a function of delay time ΔT between the IP and the DFWM beams. For $\Delta T<0$, the DFWM beams arrive at the sample first which is then followed by the IP. The DFWM beams (400 nm) are not in resonance with the ground state to an upper state transition. The signal obtained in this case is a weak nonresonant signal. Since the IP is always incident after the DFWM beams for $\Delta T<0$, it does not have any influence on the DFWM signal for negative delay times. Thus for negative delay times a constant signal is observed.

For $\Delta T>0$ the IP is incident on the sample first. The resonant IP creates a wave packet which is moving in the excited bound B state. The oscillating wave packet is probed at successive time delays by the time-coincident DFWM beams, which are resonant with the B state and ion pair state. Due to the presence of resonance a strong signal is observed. The transients exhibit well-defined oscillations with a period of 318 fs corresponding to the period of the wave packet motion in the B state. This is similar to what is observed in a pump-probe experiment where the fluorescence from the excited state is monitored. The scheme presented here, along with other advantages, also allows for the detection of nonfluorescing states. In order to analyze the data, a fast Fourier transform (FFT) of the transient in panel (a) of Fig. 2 is performed for $\Delta T>0$. The result is shown in panel (b). The FFT spectrum shows sharp peaks in the region of 105 cm^{-1}. This corresponds well to the spacing of the vibrational states, which are coherently excited in the B state of iodine by a 600 nm laser pulse.[15] Also, the second harmonic corresponding to $\Delta v=2$ can be seen at approximately 209 cm^{-1}. The experiment thus allows for the independent observation of the wave packet motion in the B state.

With the above experiment the vibrational energy spacing of the B state of iodine accessed by the 600 nm laser is determined. This will help us to discern the dynamics occurring in the B state and ion pair state in the following experiments. Further experiments were performed to observe contributions from the ion pair states. For this the IP pulse is kept fixed and made to arrive at the sample first. The delay time is chosen to be 42 ps, which means that the IP pulse arrives 42 ps earlier. Two of the DFWM pulses (DFWM pump pulses) are made to arrive simultaneously and fixed at time zero. The third (DFWM probe pulse) is varied in time (Δt). The wavelength of the DFWM beams was chosen to be 400 nm, which is in resonance with the B state and a higher lying ion pair state. As in the previous case, the IP creates a wave packet in the excited B state. The wave packet is interrogated by a time-resolved DFWM process. The transient is recorded as a function of the delay time Δt between the DFWM probe pulse and the two time-coincident DFWM pump pulses. For $\Delta t<0$ (negative delay time) the DFWM probe pulse arrives before the two time-coincident DFWM pump pulses. The transient recorded in this case is shown in panel (a) of Fig. 3. It shows a temporal structure arising from the beating between different vibrational eigenstates. The FFT spectrum of the transient for $\Delta t<0$ is shown in panel (c) of Fig. 3. Apart from the lines at 105 and 209 cm^{-1} new lines are observed at 98.9 and 197 cm^{-1}. The line at 105 cm^{-1} can be assigned to the B state vibration and its second harmonic is seen at 209 cm^{-1}. The sharp peak at 98.9 cm^{-1} arises from the ion pair states and it corresponds to the vibrational energy spacing accessed by the 400 nm laser from the B state. The less intense peak at 197 cm^{-1} is the second harmonic of this frequency.

For $\Delta t<0$, the probe pulse of the DFWM process creates a coherent superposition of several vibrational states in the higher excited state and this wave packet is interrogated by the other two DFWM pump pulses. The relevant energy level diagram for the above process is shown in panel A of Fig. 2 in the contribution by Chen *et al.*[16] The dynamics then reveal the wave packet motion in the ion pair states. However, it should be noted that for negative delay times ($\Delta t<0$) along with the excited state (ion pair states) dynamics, contributions from the lower state (B state) could also be

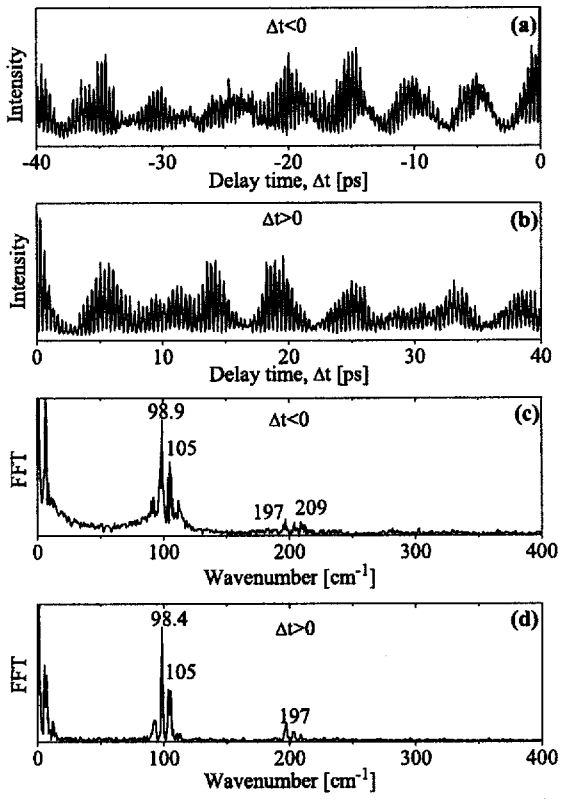

FIG. 3. DFWM transient obtained for an IP wavelength of 600 nm and a wavelength of 400 nm for the FWM laser pulses. Panels (a) and (b) show the DFWM signal recorded as a function of the delay time Δt between the two time-coincident and fixed DFWM pump pulses and the DFWM probe pulse for negative and positive delay times, respectively. The IP was made to arrive 42 ps before the two time-coincident pulses are incident on the sample. Panels (c) and (d) show the FFT spectra of the transients for $\Delta t < 0$ and $\Delta t > 0$, respectively.

observed, as is evident from Fig. 3. This is different from what is observed in earlier DFWM experiments performed on molecular iodine.[4] In those experiments, for negative delay times, only excited state (in this case, *B* state) dynamics could be observed. In the paper, the authors suggest that for strong laser pulses, a coupling of the excited and ground state coherences is possible. In our experiment, each of the DFWM pulses possessed an average energy of 2 μJ/pulse, while the IP pulse had an average energy of approximately 3.6 μJ/pulse. The DFWM laser pulses, therefore, have a relatively high intensity compared to experiments investigating the electronic ground state. In our experiments, however, a much simpler explanation can be given for the contribution of lower state dynamics (*B* state dynamics) for negative time delays. The investigation is performed on a transient population rather than a static population. The IP pulse prepares a wave packet in the excited *B* state, which oscillates back and forth. The negatively time-delayed DFWM probe pulse encounters the population prepared by the IP pulse. Since the DFWM probe pulse is varied in time, the timing between the IP pulse and the DFWM probe pulse changes. This results in the observation of the dynamics of the lower state (*B* state) for negative time delays as well. The coherent wave packet motion initiated by the IP pulse determines the overall intensity of the DFWM signal. Therefore, a variation of the timing of the DFWM probe laser pulse relative to the IP determines the possible maximum signal.

For $\Delta t > 0$ (positive delay time) the time-coincident DFWM pump pulses interact with the wave packet in the *B* state and are followed at successive time delays by the DFWM probe pulse. Panel (b) of Fig. 3 shows the dynamics for positive delay times. The FFT of the transients is taken in order to analyze the data. Panel (d) of Fig. 3 shows the FFT for positive delay times. The prominent lines appear at 98.4, 105, and 197 cm^{-1}. As in the previous case, the lines at 98.5 and 197 cm^{-1} arise from the ion pair states, while the line at 105 cm^{-1} is from the *B* state. As in previous DFWM experiments,[4] two schemes have to be considered for explaining the transients for positive delay times. The energy level diagrams for these two schemes are displayed in panels C and D of Fig. 2 in Ref. 16. For $\Delta t > 0$, the two time-coincident DFWM pump pulses prepare a wave packet in the *B* state and also in the ion pair state, which are probed by the time-delayed DFWM probe pulse. The transient thus obtained reveals the dynamics of the *B* state and the higher excited ion pair states. Here, we have to consider that the IP pulse and DFWM pump pulses are kept fixed and the DFWM probe pulse is varied in time. For positive delay times the timing between the IP pulse and the DFWM pump pulses remains constant. Therefore, for $\Delta t > 0$, the *B* state contribution is only due to the wave packet prepared by the two DFWM pump pulses in the *B* state.

In order to verify that the contributions observed in the FFT are from the ion pair states, additional experiments were performed. The wavelength of the initial pump was kept fixed at 600 nm, while the wavelengths of the FWM beams were varied. A constant IP wavelength means that the same vibrational levels of the *B* state are excited. Now, by changing the wavelengths of the DFWM beams, higher or lower energy regions of the PES of the ion pair states can be accessed. This change should be reflected in the transients recorded. The results of the corresponding experiments are presented below.

As for a first case, the wavelength of the FWM beams was changed to 380 nm. The dynamics were recorded as in the previous case. As before, the IP was made to arrive 42 ps earlier. The probe pulse of the DFWM process was varied between $\Delta t = -40$ (negative delay times) and +40 ps (positive delay time), keeping the two DFWM pump pulses temporally overlapped and fixed at time zero. The recorded dynamics for negative and positive delay times are shown in panels (a) and (b) of Fig. 4, respectively. The FFTs of the transients in panels (a) and (b) are shown in panels (c) and (d), respectively. The FFT spectrum in panel (c) of the transient obtained for negative delay times shows sharp peaks at 93 and at 104 and 107 cm^{-1}. The line at 93 cm^{-1} clearly belongs to the ion pair state and the 104 and 107 cm^{-1} lines can be assigned to the *B* state wave packet motion. For positive delay times also, the contribution from the ion pair state is evident from the line at 92.5 cm^{-1}, as seen from panel (d) of Fig. 4. When compared to the experiments performed with a FWM wavelength of 400 nm, the lines are shifted to the low wavenumber side for 380 nm. This is according to the ex-

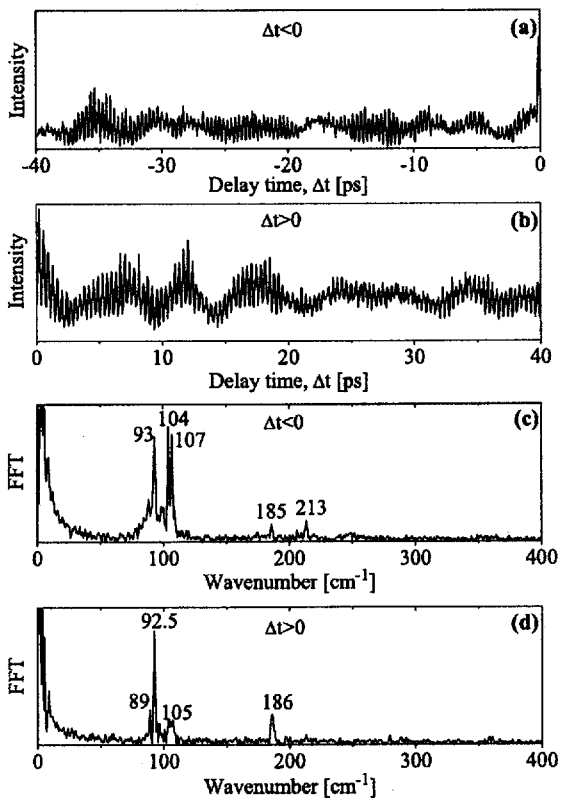

FIG. 4. DFWM transient obtained for an IP wavelength of 600 nm and a wavelength of 380 nm for the FWM laser pulses. Panels (a) and (b) show the DFWM signal recorded as a function of the delay time Δt between the two time-coincident and fixed DFWM pump pulses and the DFWM probe pulse for negative and positive delay times, respectively. The IP was made to arrive 42 ps before the two time-coincident pulses are incident on the sample. Panels (c) and (d) show the FFT spectra of the transients for $\Delta t < 0$ and $\Delta t > 0$, respectively.

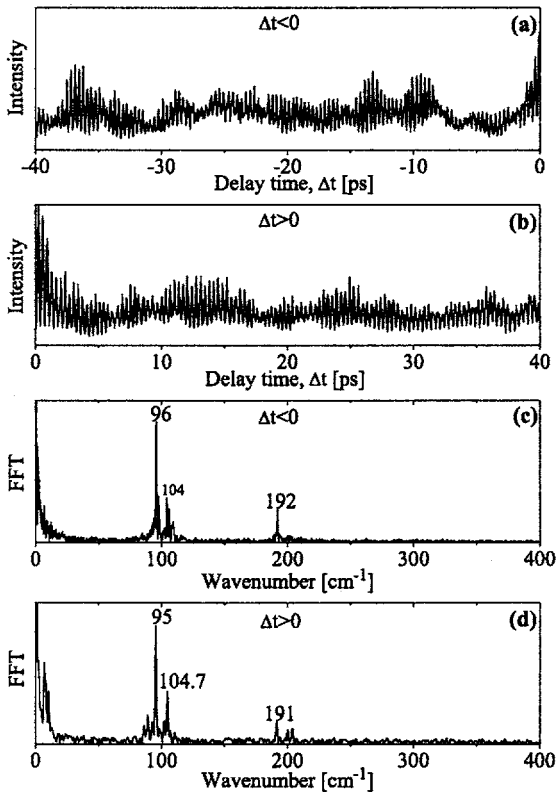

FIG. 5. DFWM transient obtained for an IP wavelength of 600 nm and a wavelength of 390 nm for the FWM laser pulses. Panels (a) and (b) show the DFWM signal recorded as a function of the delay time Δt between the two time-coincident and fixed DFWM pump pulses and the DFWM probe pulse for negative and positive delay times, respectively. The IP was made to arrive 42 ps before the two time-coincident pulses are incident on the sample. Panels (c) and (d) show the FFT spectra of the transients for $\Delta t < 0$ and $\Delta t > 0$, respectively.

pectations since shorter wavelengths access higher vibrational energy states, where the vibrational spacing becomes smaller due to the anharmonicity of the potential curve.

As before, for negative time delays, the B state signal is also observed. This can be understood from what was explained before. The varying timing between the IP pulse and the DFWM probe pulse leads to the observation of the B state signal. Since the wave packet prepared by the IP yields the population available for the DFWM process, the variation of the IP-DFWM time delay modulates the signal with very high efficiency. For positive time delays, the time delay between the IP and the DFWM pump pulses does not vary. Our transients yield a rather small B state contribution compared to the ion pair state signal [see FFT spectrum shown in panel (d) of Fig. 4]. As already stated in the publication by Schmitt *et al.*,[4] the contribution of the B state observed in the FFT spectrum is for the present case exclusively determined by the Franck-Condon overlaps involved in the corresponding Feynman diagrams, which describe the nonlinear interaction. Also, if we look into the previous DFWM results displayed in Fig. 2 of Ref. 4, it can be found that for positive time delays, the contribution from the ground X state is rather weak compared to the excited B state contribution.

Figure 5 shows the transients recorded and corresponding FFT spectra for an IP wavelength of 600 nm and a FWM wavelength of 390 nm. With a DFWM wavelength of 390 nm lower energy regions of the ion pair states should be accessed compared to 380 nm. Here, the vibrational energy spacing should be larger than that is observed for 380 nm. Panels (a) and (b) show the dynamics for negative and positive time delays, respectively. The FFT of the transient for negative time delay shown in panel (c) exhibits peaks at 96, 104, and 192 cm^{-1}. The line at 104 cm^{-1} is the B state vibrational spacing, which is seen due to the varying time delay between the IP pulse and the DFWM probe pulse. The peak at 96 cm^{-1} is the vibrational energy spacing of the ion pair state and the second harmonic is seen at 192 cm^{-1}. This corresponds well to expectations where at 390 nm, the vibrational energy spacing is larger than that reached by 380 nm laser, while it is smaller than that accessed by 400 nm laser. The FFT for $\Delta t > 0$ shows the B state vibrational energy spacing at 104.7 cm^{-1} and the ion pair state spacing at 95 cm^{-1}. Again, the explanations given above are consistent with the observations.

Now, the DFWM wavelength is further changed to the longer wavelength region at 410 nm. As in the previous experiments, the IP arrives 42 ps earlier. The transients are recorded by varying the DFWM probe pulse from −40 to 40 ps. This is shown in panels (a) and (b) of Fig. 6 for $\Delta t < 0$ and $\Delta t > 0$, respectively. DFWM at 410 nm accesses lower regions of the PES where the vibrational energy

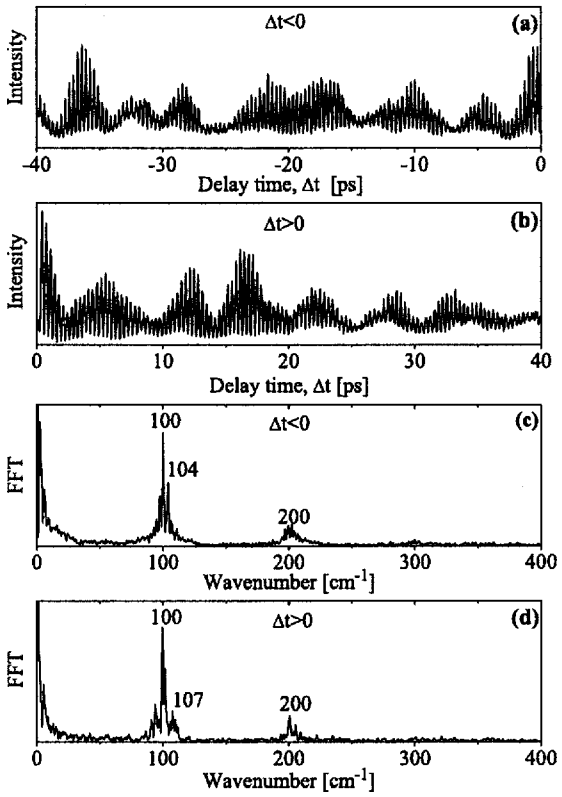

FIG. 6. DFWM transient obtained for an IP wavelength of 600 nm and a wavelength of 410 nm for the FWM laser pulses. Panels (a) and (b) show the DFWM signal recorded as a function of the delay time Δt between the two time-coincident and fixed DFWM pump pulses and the DFWM probe pulse for negative and positive delay times, respectively. The IP was made to arrive 42 ps before the two time-coincident pulses are incident on the sample. Panels (c) and (d) show the FFT spectra of the transients for $\Delta t<0$ and $\Delta t>0$, respectively.

spacing is larger. So we expect a larger wavenumber spacing at 410 nm than that is observed at 400 nm. The FFT of the transient for negative time delay is displayed in panel (c) of Fig. 6. It shows lines at 100, 104, and small peaks in the region of 200 cm^{-1}. The contributions at 100 and 200 cm^{-1} are from the ion pair state, while the peak at 104 cm^{-1} is from the B state. The transients clearly show the contribution from the ion pair states shifted in the predicted way. The FFT for $\Delta t>0$ is shown in panel (d) of Fig. 6. The B state contribution prepared by the two DFWM pump pulses acting simultaneously is seen at 107 cm^{-1}. The line at 100 cm^{-1} is the vibrational energy spacing of the ion pair state. The second harmonic is seen at 200 cm^{-1}.

Even though it is possible to monitor the wave packet motion in the ion pair states, it is not absolutely clear whether the contribution is from the $\beta(1g)$ or from the $E(0_g^+)$ state. These states have very similar molecular parameters and both are accessible from the B state with the wavelengths used for the DFWM process. However, the transition to the $\Omega=1$ state is approximately 30 times weaker than the $\Delta\Omega=0$ transition from the B to the E state.[17,18] Therefore, we assume that in our experiments, from among the ion pair states, the contributions from the $E(0_g^+)$ state are dominating in the transient. Although it is a possibility that a beating between $\beta(1g)$ and $E(0_g^+)$ occurs, it is highly unlikely due to the above factor that we observe it in the transient.

IV. CONCLUSIONS

A combination of an initial pump excitation and a time-resolved DFWM probe process proves to be a valuable technique in exploring the dynamics of higher excited states of molecules. The versatility of the technique has been demonstrated in the case of iodine where dynamics of the higher lying ion pair states along with the dynamics of the excited B state have been monitored. This was achieved by analyzing the DFWM signal as a function of the delay time between one of the three FWM laser pulses and the other two time-coincident pump pulses. We demonstrated that by changing the wavelength of the DFWM beams different regions of the PES could be accessed, thereby confirming the ion pair state contribution to the dynamics. Using this technique, a mapping of the ion pair state PESs is possible.

ACKNOWLEDGMENTS

The authors thank Dr. Torsten Balster for his continuous help with the measuring software. This work has been supported by the German Research Foundation (DFG, Grant No. MA 1564/13-1,2).

[1] R. M. Bowman, M. Dantus, and A. H. Zewail, Chem. Phys. Lett. **161**, 297 (1989).
[2] M. Dantus, R. M. Bowman, and A. H. Zewail, Nature (London) **343**, 737 (1990).
[3] M. Schmitt, G. Knopp, A. Materny, and W. Kiefer, Chem. Phys. Lett. **270**, 9 (1997).
[4] M. Schmitt, G. Knopp, A. Materny, and W. Kiefer, Chem. Phys. Lett. **280**, 339 (1997).
[5] G. Knopp, I. Pinkas, and Y. Prior, J. Raman Spectrosc. **31**, 51 (2000).
[6] T. Siebert, M. Schmitt, A. Vierheilig, G. Flachenecker, V. Engel, A. Materny, and W. Kiefer, J. Raman Spectrosc. **31**, 25 (2000).
[7] R. M. Bowman, M. Dantus, and A. H. Zewail, Chem. Phys. Lett. **174**, 546 (1990).
[8] P. Farmanara, H.-H. Ritze, V. Stert, and W. Radloff, Chem. Phys. Lett. **307**, 1 (1999).
[9] M. Motzkus, S. Pedersen, and A. H. Zewail, J. Phys. Chem. **100**, 5620 (1996).
[10] A. C. Eckbreth, Appl. Phys. Lett. **32**, 421 (1978).
[11] G. W. King, I. M. Littlewood, and J. R. Robbins, Chem. Phys. **56**, 145 (1981).
[12] J. P. Perrot, M. Broyer, J. Chevaleyre, and B. Femelat, J. Mol. Spectrosc. **98**, 161 (1983).
[13] M. D. Danyluk and G. W. King, Chem. Phys. **22**, 59 (1977).
[14] A. D. Williamson, Chem. Phys. Lett. **60**, 451 (1979).
[15] R. F. Barrow and K. K. Yee, J. Chem. Soc., Faraday Trans. 2 **69**, 684 (1973).
[16] T. Chen, V. Engel, M. Heid, W. Kiefer, G. Knopp, A. Materny, S. Meyer, R. Pausch, M. Schmitt, H. Schwoerer, and T. Siebert, J. Mol. Struct. **480**, 33 (1999).
[17] J. P. Perrot, B. Femelat, J. L. Subtil, M. Broyer, and J. Chevaleyre, Mol. Phys. **61**, 85 (1987).
[18] J. P. Perrot, B. Femelat, M. Broyer, and J. Chevaleyre, Mol. Phys. **61**, 97 (1987).